Національна академія наук України

ІНСТИТУТ
ФІЗИКИ
КОНДЕНСОВАНИХ
СИСТЕМ

ICMP–18–05E

V. Baliha, J. Richter,* O. Derzhko

GROUND-STATE PHASES OF FRUSTRATED BILAYER QUANTUM HEISENBERG ANTIFERROMAGNETS

*Institut für theoretische Physik, Otto-von-Guericke-Universität Magdeburg, P.O. Box 4120, 39016 Magdeburg, Germany

ЛЬВІВ

УДК: 537.9, 537.622

PACS: 75.10.-b, 75.10.Jm

Фази в основному стані квантового антиферомагнетика Гайзенберга на фрустрованих двошарах

В. Балiга, Й. Рiхтер, О. Держко

Анотацiя. Ми використовуємо варiацiйний середньопольовий пiдхiд для побудови фазової дiаграми в основному станi антиферомагнетика Гайзенберга на фрустрованих квадратних i шестикутних двошарах. Нашi результати є у добрiй згодi з результатами складнiших пiдходiв.

Ground-state phases of frustrated bilayer quantum Heisenberg antiferromagnets

V. Baliha, J. Richter, O. Derzhko

Abstract. We use a variational mean-field approach to construct the ground-state phase diagram of the Heisenberg antiferromagnet on the square-lattice and honeycomb-lattice bilayers. Our findings are in a good agreement with the results of more sophisticated approaches.

Препринти Інституту фізики конденсованих систем НАН України розповсюджуються серед наукових та інформаційних установ. Вони також доступні по електронній комп'ютерній мережі на WWW-сервері інституту за адресою http://www.icmp.lviv.ua/

The preprints of the Institute for Condensed Matter Physics of the National Academy of Sciences of Ukraine are distributed to scientific and informational institutions. They also are available by computer network from Institute's WWW server (http://www.icmp.lviv.ua/)

Василь Ярославович Баліга
Йоганнес Ріхтер
Олег Володимирович Держко

Фази в основному стані квантового антиферомагнетика Гайзенберга на фрустрованих двошарах

Роботу отримано 12 листопада 2018 р.

Затверджено до друку Вченою радою ІФКС НАН України

Рекомендовано до друку відділом квантової статистики

Виготовлено при ІФКС НАН України

Bilayer quantum ($s = 1/2$) Heisenberg antiferromagnets are defined by the Hamiltonian

$$H = \sum_{\langle pq \rangle} J_{pq} \mathbf{s}_p \cdot \mathbf{s}_q, \tag{1}$$

where the sum runs over the exchange interaction pattern of the corresponding bilayer lattice, see Fig. 1 for the instances of the square-lattice bilayer (left) and the honeycomb-lattice bilayer (right). The bilayer lattice consists of $N = 2\mathcal{N}$ sites, where $\mathcal{N}$ is the number of vertical dimers (i.e., the number of the lattice sites of the underlying lattice). The underlying lattices for the cases to be considered here are bipartite ones, i.e., they consist of two sublattices, say A and B. For the square-lattice case, we may assume that the sublattice-A site indexes are $r = (i, j)$ and $i + j$ is even, whereas the sublattice-B site indexes are $r = (i, j)$ and $i+j$ is odd. Moreover, each vertical dimer connects the nearest-neighbor sites from the top layer t and the bottom layer b.

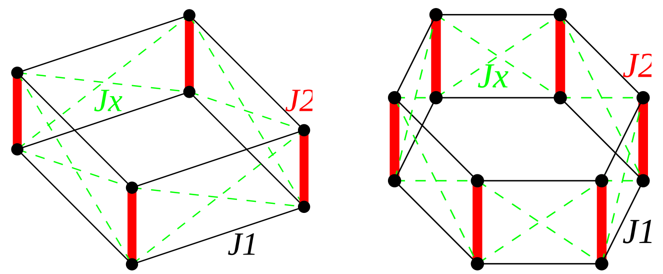

Figure 1. Square- and honeycomb-lattice bilayers considered in the present paper. Each vertical dimer connects the nearest-neighbor sites from the top layer t and the bottom layer b. Thick solid red lines correspond to the exchange couplings J_2 (nearest-neighbor interlayer coupling), thin solid black lines correspond to the exchange couplings J_1 (nearest-neighbor intralayer coupling), and thin dashed green lines correspond to the exchange couplings $J_\times$ (next-nearest-neighbor interlayer coupling).

Bilayer quantum Heisenberg antiferromagnets have received some interest nowadays not only because of experimental relevance [1–3], but also because of a possibility to realize high-precision quantum Monte Carlo simulations which are sign-free in the presence of perfect frustration [4–7]. We may also mention here several recent studies on the low-temperature thermodynamics of the frustrated quantum Heisenberg bilayers given by Eq. (1) [8–10] as well as of such systems in the presence of a magnetic field [11–14], when the Hamiltonian (1) contains in addition the Zeeman term $-h\sum_p s_p^z$.

In what follows, we focus on the ground-state phase diagram of the square- and honeycomb-lattice bilayers (1) parameterized by three different exchange interactions, namely, by the nearest-neighbor interlayer coupling J_2, the nearest-neighbor intralayer coupling J_1, and the next-nearest-neighbor interlayer coupling $J_\times$. The phase diagram of the square-lattice bilayer has been obtained in Ref. [6] by the method of infinite projected entangled pair states, whereas the phase diagram of the honeycomb-lattice bilayer has been obtained in Ref. [8] by a set of complementary approaches, namely, Schwinger bosons, dimer series expansion, bond operators, and exact diagonalization. Below we show that these ground-state phase diagrams can be reproduced reasonably well by a simple variational approach explained in detail in Refs. [15–19] (see also Ref. [20]).

We begin with the square-lattice bilayer. It possesses the following symmetry: The change of labeling $t \leftrightarrow b$ on one of two sublattices of the underlying square lattice (e.g., on the sublattice B with the site indexes $r=(i,j)$, $i+j$ is odd) leads to the interchange of the exchange interactions $J_1 \leftrightarrow J_\times$, see Fig. 1. As a result, we may restrict ourselves to the case $J_1 \le J_\times$ and obtain the results for the opposite case $J_1 \ge J_\times$ by symmetry.

Assume at first $J_1 \ll J_\times$. In the small-J_2 limit one faces two noninteracting square lattices with the antiferromagnetic Néel-type long-range order and in the large-J_2 limit one faces the regular pattern of singlets (on the vertical bonds), which is called valence-bond state. Then the trial wave function

$$|\Gamma\rangle = \prod_r \left(\frac{|\uparrow_t\downarrow_b\rangle - \Gamma|\downarrow_t\uparrow_b\rangle}{\sqrt{1+\Gamma^2}}\right)_r, \tag{2}$$

where $r=(i,j)$ runs over all $\mathcal{N}$ vertical bonds (dimers) and $0 \le \Gamma \le 1$ interpolates between the Néel-like order (to be called bilayer antiferromagnet order (BAF)) for $0 \le \Gamma < 1$ and the dimer singlet order (DS) for $\Gamma = 1$. After straightforward calculations using (2) one gets the variational energy

$$\frac{E(\Gamma)}{\mathcal{N}} = -\left(\frac{1}{4} + \frac{\Gamma}{1+\Gamma^2}\right) J_2 + \left(\frac{1-\Gamma^2}{1+\Gamma^2}\right)^2 (J_1 - J_\times) \tag{3}$$

and the optimal value of the variational parameter Γ

$$\Gamma = \begin{cases} 1, & \text{if} \quad 4(J_\times - J_1) \le J_2, \\ \frac{4(J_\times - J_1)}{J_2} - \sqrt{\frac{16(J_\times - J_1)^2}{J_2^2} - 1}, & \text{if} \quad 4(J_\times - J_1) \ge J_2. \end{cases} \tag{4}$$

The behavior of the on-site magnetization with varying J_2 indicates a continuous (second-order) quantum phase transition.

Next, assume $J_1 \approx J_\times$. In the case of perfect frustration $J_1 = J_\times$ the model has local integrals of motion (the total spin at each vertical bond). In the small-J_2 limit one faces the regular pattern of triplets on the vertical bonds and in the large-J_2 limit one faces the regular pattern of singlets on the vertical bonds (valence-bond state). Then we introduce the following trial wave function

$$|\beta\rangle = \prod_r \left(\beta|DS\rangle + \sqrt{1-\beta^2}|DTAF\rangle\right)_r,$$
$$|DS\rangle_r = \frac{|\uparrow_t\downarrow_b\rangle - |\downarrow_t\uparrow_b\rangle}{\sqrt{2}},$$
$$|DTAF\rangle_r = \frac{1+(-1)^{i+j}}{2}|\uparrow_t\uparrow_b\rangle + \frac{1-(-1)^{i+j}}{2}|\downarrow_t\downarrow_b\rangle, \tag{5}$$

where $0 \le \beta \le 1$. $|\beta\rangle$ (5) illustrates a competition between the dimer singlet phase (if $\beta = 1$) and the dimer triplet antiferromagnet ($DTAF$) phase (if $\beta = 0$). It yields the variational energy

$$\frac{E(\beta)}{\mathcal{N}} = \left(\frac{1}{4} - \beta^2\right) J_2 - 2\left(1-\beta^2\right)\beta^2 (J_1 - J_\times) - \left(1-\beta^2\right)^2 (J_1 + J_\times). \tag{6}$$

For the optimal value of β we have:

$$\beta = \begin{cases} 1, & \text{if} \quad J_\times + J_1 \le J_2, \\ 0, & \text{if} \quad J_\times + J_1 \ge J_2. \end{cases} \tag{7}$$

The behavior of the on-site magnetization with varying J_2 indicates a discontinuous (first-order) quantum phase transition.

To complete the variational analysis of the ground state, we have to compare the energy of the BAF phase with the energy of the $DTAF$ phase in the region $J_\times/J_2 \ge J_1/J_2 + 1/4$. One immediately concludes that the $DTAF$ phase has lower energy only for $J_1/J_2 > 1/4$ and $J_\times/J_2 > [32(J_1/J_2)^2 - 8J_1/J_2 + 1]/(32J_1/J_2 - 8)$.

Combining all results together, we arrive at the ground-state phase diagram for the square-lattice bilayer shown in Fig. 2 (in the plane

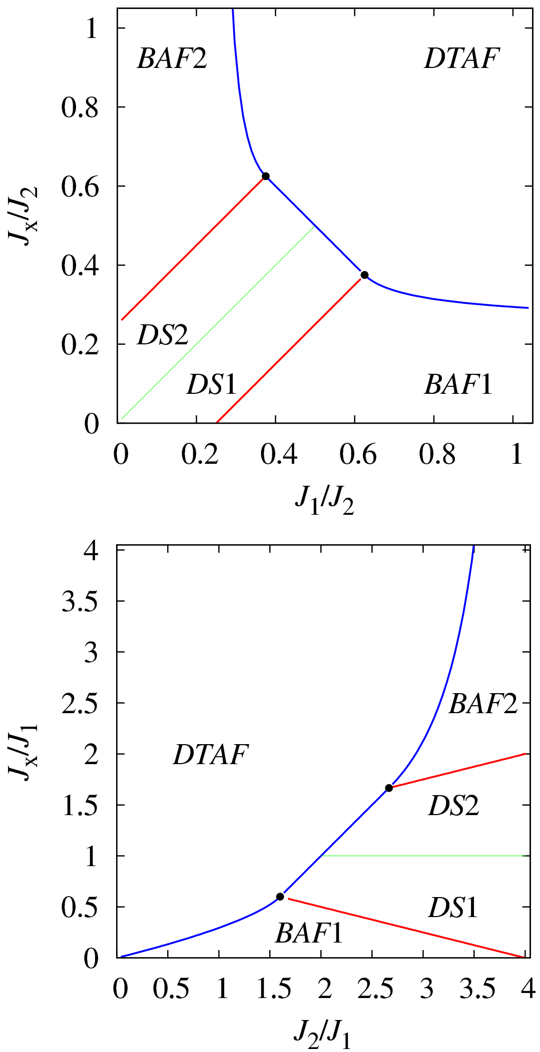

Figure 2. Ground-state phase diagram for the square-lattice bilayer obtained within the variational mean-field approach in the $J_1/J_2 - J_\times/J_2$ plane (top) and in the $J_2/J_1 - J_\times/J_1$ plane (bottom). Red (blue) curves correspond to continuous (discontinuous) quantum phase transitions. Black circles denote quantum triple points.

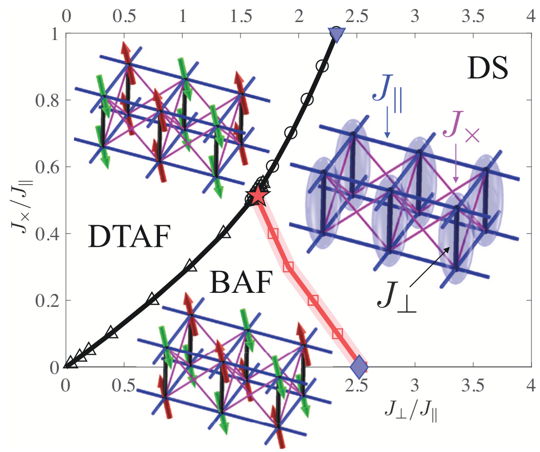

Figure 3. The ground-state phase diagram for the square-lattice bilayer taken from Ref. [6]. It has to be compared with Fig. 2, bottom, where the lower part of the diagram corresponds to $J_\times/J_1 \leq 1$.

$J_1/J_2 - J_\times/J_2$ (top) and in the plane $J_2/J_1 - J_\times/J_1$ (bottom)). The part of the phase diagram which corresponds to the case $J_1 \geq J_\times$ has been added by symmetry. The obtained ground-state phase diagram contains several magnetic (BAF and $DTAF$) and nonmagnetic (DS) phases, continuous phase transition lines (red), discontinuous phase transition lines (blue), and two triple points (black circles).

For $J_\times = 0$ (unfrustrated square-lattice bilayer), the transition between the $BAF1$ and $DS1$ phases occurs at $J_2/J_1 = 4$ (Ref. [6] reports the value 2.5220(2); the earlier variational paper [15] obviously gives also 4; quantum Monte Carlo simulations [21] yield 2.5220(1)). For $J_\times = J_1$ (fully frustrated square-lattice bilayer), the transition between the $DTAF$ and DS phases occurs at $J_2/J_1 = 2$ (Ref. [6] reports the value 2.3279(1)). Two triple points in Fig. 2, top with the coordinates $(3/8, 5/8)$ and $(5/8, 3/8)$ imply that the $DTAF$, $BAF1$, and $DS1$ phases meet at $J_2 = 8J_1/5 = 1.6J_1$ and $J_\times = 3J_1/5 = 0.6J_1$. These numbers can be compared to the results of Ref. [6]: $J_2 = 1.638(15)J_1$ and $J_\times = 0.520(5)J_1$. Overall, as it follows from a comparison of Figs. 2 and 3, the simple variational mean-field approach provides quite reasonable agreement with the outcomes of more sophisticated methods, see [6, 15, 21] and references therein.

In the case of the honeycomb-lattice bilayer, the ground-state phase

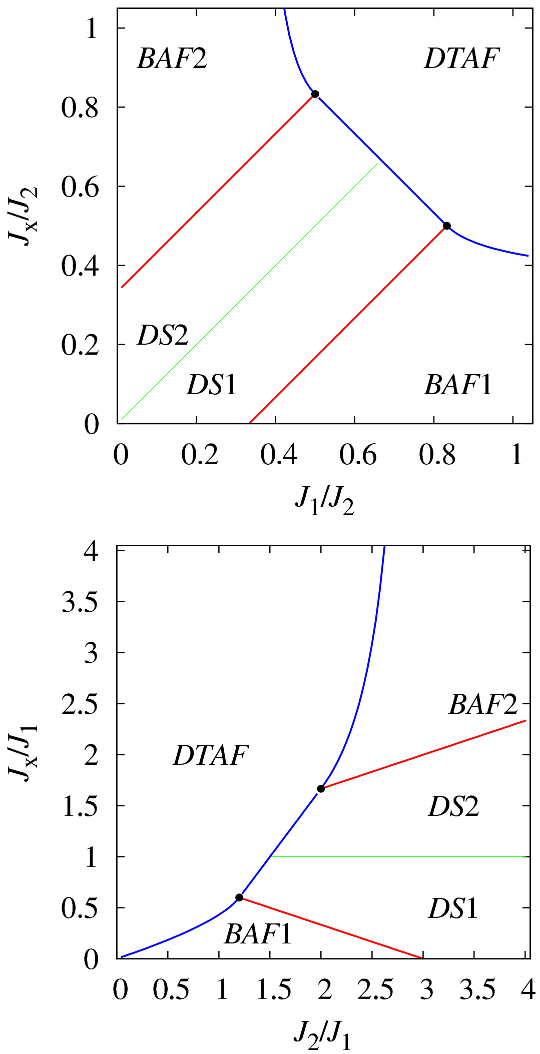

Figure 4. Ground-state phase diagram for the honeycomb-lattice bilayer obtained within the variational mean-field approach in the $J_1/J_2 - J_x/J_2$ plane (top) and in the $J_2/J_1 - J_x/J_1$ plane (bottom). Red (blue) curves correspond to continuous (discontinuous) quantum phase transitions. Black circles denote quantum triple points.

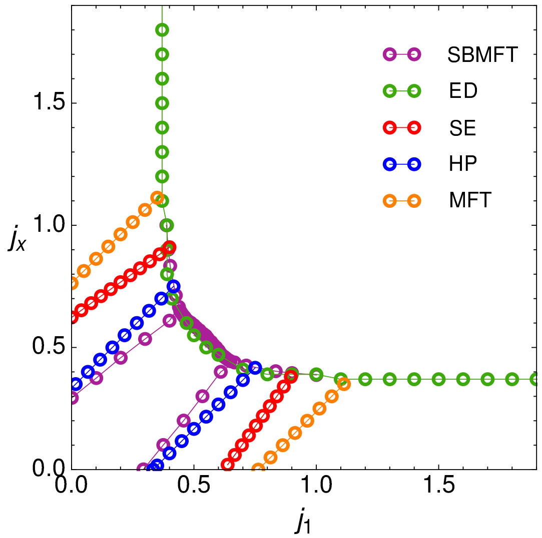

Figure 5. The ground-state phase diagram for the honeycomb-lattice bilayer taken from Ref. [8]. It has to be compared with Fig. 4, top.

diagram shown in Fig. 4 remains qualitatively as in the case of the square-lattice bilayer, however, quantitative details are different because of a different number of the neighboring vertical dimer bonds. The honeycomb-lattice bilayer has been examined in Ref. [8] and we may use the results of this paper to corroborate our variational calculations. For a critical point on the $J_1 = J_x$ line Ref. [8] gives: $(J_1/J_2)_c^{\rm SB-MFT} = 0.547$ and $(J_1/J_2)_c^{\rm LSWT} = 0.551$. Our prediction is: $(J_1/J_2)_c = 2/3 \approx 0.667$. For the coordinates of the quantum triple points we have: $J_1/J_2 = 1/2 = 0.5$, $J_x/J_2 = 5/6 = 0.833\ldots$ and $J_1/J_2 = 5/6 = 0.833\ldots$, $J_x/J_2 = 1/2 = 0.5$. To compare further details of our phase diagram with the results of Ref. [8], see Figs. 4 and 5.

In conclusion, the described variational mean-field approach allows one to obtain in a simple manner the ground-state phase diagram for the square- and honeycomb-lattice frustrated bilayers. More intriguing question is the triangular- and kagome-lattice frustrated bilayers. The work in this direction is in progress.

Acknowledgments

V. B. was partially supported by the National Academy of Sciences of Ukraine under Grant for the Research groups of young scientists (Contract No. 17/2018). J. R. and O. D. thank the Wilhelm und Else Heraeus Stiftung for the kind hospitality at the 673. WE-Heraeus-Seminar "Trends in Quantum Magnetism" (Bad Honnef, 4-8 June 2018). O. D. acknowledges the kind hospitality of the MPIPKS, Dresden in April-June and September of 2018 and at the Workshop "Correlated Electrons in Transition-Metal Compounds: New Challenges" (5-9 November 2018). The work of O. D. was partially supported by Project FF-30F (No. 0116U001539) from the Ministry of Education and Science of Ukraine.

References

1. H. Tanaka, N. Kurita, M. Okada, E. Kunihiro, Y. Shirata, K. Fujii, H. Uekusa, A. Matsuo, K. Kindo, and H. Nojiri, "Almost perfect frustration in the dimer magnet $Ba_2CoSi_2O_6Cl_2$", J. Phys. Soc. Jpn. **83**, 103701 (2014).
2. O. Smirnova, M. Azuma, N. Kumada, Y. Kusano, M. Matsuda, Y. Shimakawa, T. Takei, Y. Yonesaki, and N. Kinomura, "Synthesis, crystal structure, and magnetic properties of $Bi_3Mn_4O_{12}(NO_3)$ oxynitrate comprising $S = 3/2$ honeycomb lattice", J. Am. Chem. Soc. **131**, 8313 (2009); S. Okubo, F. Elmasry, W. Zhang, M. Fujisawa, T. Sakurai, H. Ohta, M. Azuma, O. A. Sumirnova, and N. Kumada, "High-field ESR measurements of $S = 3/2$ honeycomb lattice antiferromagnet $Bi_3Mn_4O_{12}(NO_3)$", J. Phys.: Conf. Ser. **200**, 022042 (2010); M. Matsuda, M. Azuma, M. Tokunaga, Y. Shimakawa, and N. Kumada, "Disordered ground state and magnetic field-induced long-range order in an $S = 3/2$ antiferromagnetic honeycomb lattice compound $Bi_3Mn_4O_{12}(NO_3)$", Phys. Rev. Lett. **105**, 187201 (2010); H. C. Kandpal and J. van den Brink, "Calculation of magnetic exchange couplings in the $S = 3/2$ honeycomb system $(Bi_3Mn_4O_{12})NO_3$ from first principles", Phys. Rev. B **83**, 140412(R) (2011); M. Alaei, H. Mosadeq, I. A. Sarsari, and F. Shahbazi, "Origin of magnetic frustration in $Bi_3Mn_4O_{12}(NO_3)$", Phys. Rev. B **96**, 140404(R) (2017).
3. J. M. Ni, Q. Y. Liu, Y. J. Yu, E. J. Cheng, Y. Y. Huang, Z. Y. Liu, X. J. Wang, Y. Sui, and S. Y. Li, "Ultralow-temperature heat transport in the quantum spin liquid candidate $Ca_{10}Cr_7O_{28}$ with a bilayer kagome lattice", Phys. Rev. B **97**, 104413 (2018).
4. F. Alet, K. Damle, and S. Pujari, "Sign-problem-free Monte Carlo simulation of certain frustrated quantum magnets", Phys. Rev. Lett. **117**, 197203 (2016).
5. S. Wessel, B. Normand, F. Mila, and A. Honecker, "Efficient quantum Monte Carlo simulations of highly frustrated magnets: The frustrated spin-1/2 ladder", SciPost Phys. **3**, 005 (2017).
6. J. Stapmanns, P. Corboz, F. Mila, A. Honecker, B. Normand, and S. Wessel, "Thermal critical points and quantum critical end point in the frustrated bilayer Heisenberg antiferromagnet", Phys. Rev. Lett. **121**, 127201 (2018).
7. S. Wessel, I. Niesen, J. Stapmanns, B. Normand, F. Mila, P. Corboz, and A. Honecker, "Thermodynamic properties of the Shastry-Sutherland model from quantum Monte Carlo simulations", arXiv:1808.02043.
8. H. Zhang, C. A. Lamas, M. Arlego, and W. Brenig, "Quantum phase diagram of a frustrated antiferromagnet on the bilayer honeycomb lattice", Phys. Rev. B **93**, 235150 (2016).
9. H. Zhang, C. A. Lamas, M. Arlego, and W. Brenig, "Nematic quantum phases in the bilayer honeycomb antiferromagnet", Phys. Rev. B **97**, 235123 (2018).
10. R. F. Bishop and P. H. Y. Li, "Frustrated honeycomb-bilayer Heisenberg antiferromagnet: The spin-$\frac{1}{2}$ $J_1 - J_2 - J_1^{\perp}$ model", Phys. Rev. B **95**, 134414 (2017); R. F. Bishop and P. H. Y. Li, "High-order study of the quantum critical behavior of a frustrated spin-$\frac{1}{2}$ antiferromagnet on a stacked honeycomb bilayer", Phys. Rev. B **96**, 224416 (2017).
11. J. Richter, O. Derzhko, and T. Krokhmalskii, "Finite-temperature order-disorder phase transition in a frustrated bilayer quantum Heisenberg antiferromagnet in strong magnetic fields", Phys. Rev. B **74**, 144430 (2006); O. Derzhko, T. Krokhmalskii, and J. Richter, "Emergent Ising degrees of freedom in frustrated two-leg ladder and bilayer $s = \frac{1}{2}$ Heisenberg antiferromagnets", Phys. Rev. B **82**, 214412 (2010); J. Richter, O. Krupnitska, V. Baliha, T. Krokhmalskii, and O. Derzhko, "Thermodynamic properties of $Ba_2CoSi_2O_6Cl_2$ in strong magnetic field: Realization of flat-band physics in a highly frustrated quantum magnet", Phys. Rev. B **97**, 024405 (2018).
12. F. A. Gómez Albarracin and H. D. Rosales, "Field-induced multiple order-by-disorder state selection in an antiferromagnetic honeycomb bilayer lattice", Phys. Rev. B **93**, 144413 (2016).
13. T. Krokhmalskii, V. Baliha, O. Derzhko, J. Schulenburg, and

J. Richter, "Frustrated honeycomb-lattice bilayer quantum antiferromagnet in a magnetic field: Unconventional phase transitions in a two-dimensional isotropic Heisenberg model", Phys. Rev. B **95**, 094419 (2017); T. Krokhmalskii, V. Baliha, O. Derzhko, J. Schulenburg, and J. Richter, "Frustrated honeycomb-lattice bilayer quantum antiferromagnet in a magnetic field", Physica B **536**, 388 (2018).
14. J. Strečka, K. Karľová, V. Baliha, and O. Derzhko, "Ising versus Potts criticality in low-temperature magnetothermodynamics of a frustrated spin-$\frac{1}{2}$ Heisenberg triangular bilayer", arXiv:1807.08042, to appear in Phys. Rev. B **98**, (2018).
15. C. Gros, W. Wenzel, and J. Richter, "The transition from an ordered antiferromagnet to a quantum disordered spin liquid in a solvable bilayer model", Europhys. Lett. **32**, 747 (1995).
16. S. E. Krüger, J. Richter, J. Schulenburg, D. J. J. Farnell, and R. F. Bishop, "Quantum phase transitions of a square-lattice Heisenberg antiferromagnet with two kinds of nearest-neighbor bonds: A high-order coupled-cluster treatment", Phys. Rev. B **61**, 14607 (2000).
17. J. Richter, J. Schulenburg, A. Honecker, and D. Schmalfuß, "Absence of magnetic order for the spin-half Heisenberg antiferromagnet on the star lattice", Phys. Rev. B **70**, 174454 (2004).
18. *Quantum Magnetism*, Lecture Notes in Physics **645**, edited by U. Schollwöck, J. Richter, D. J. J. Farnell, and R. F. Bishop (Springer, Berlin, 2004).
19. J. Richter and O. Derzhko, "Quantum phase transitions: A variational mean-field perspective", European Journal of Physics **38**, 033002 (2017).
20. V. M. Kalita and V. M. Loktev, "On the theory of the magnetization of dimerized magnets", JETP Letters **91**, 183 (2010); V. M. Kalita and V. M. Loktev, "Theory of quantum phase transitions in dimerized antiferromagnets", Low Temperature Physics **36**, 665 (2010).
21. Ling Wang, K. S. D. Beach, and Anders W. Sandvik, "High-precision finite-size scaling analysis of the quantum-critical point of $S = 1/2$ Heisenberg antiferromagnetic bilayers", Phys. Rev. B **73**, 014431 (2006); L. Fritz, R. L. Doretto, S. Wessel, S. Wenzel, S. Burdin, and M. Vojta, "Cubic interactions and quantum criticality in dimerized antiferromagnets", Phys. Rev. B **83**, 174416 (2011).

CONDENSED MATTER PHYSICS

The journal **Condensed Matter Physics** is founded in 1993 and published by Institute for Condensed Matter Physics of the National Academy of Sciences of Ukraine.

AIMS AND SCOPE: The journal **Condensed Matter Physics** contains research and review articles in the field of statistical mechanics and condensed matter theory. The main attention is paid to physics of solid, liquid and amorphous systems, phase equilibria and phase transitions, thermal, structural, electric, magnetic and optical properties of condensed matter. Condensed Matter Physics is published quarterly.

ABSTRACTED/INDEXED IN: Chemical Abstract Service, Current Contents/Physical, Chemical&Earth Sciences; ISI Science Citation Index-Expanded, ISI Alerting Services; INSPEC; "Referatyvnyj Zhurnal"; "Dzherelo".

CONTACT INFORMATION:
Institute for Condensed Matter Physics
of the National Academy of Sciences of Ukraine
1 Svientsitskii Str., 79011 Lviv, Ukraine
Tel: +38(032)2761978; Fax: +38(032)2761158
E-mail: cmp@icmp.lviv.ua   http://www.icmp.lviv.ua